Pergamon

Corrosion Science, Vol. 39, No. 9, pp. 1531–1543, 1997

0010-938X/97 $17.00 + 0.00

PII: S0010-938X(97)00052-8

THE EFFECT OF INDIUM IMPURITY ON THE DC-ETCHING BEHAVIOUR OF ALUMINUM FOIL FOR ELECTROLYTIC CAPACITOR USAGE

W. LIN,* G. C. TU,* C. F. LIN† and Y. M. PENG†

* Institute of Materials Science and Engineering, National Chiao Tung University, Hsinchu, Taiwan, R.O. China
† Materials Research Laboratories, Industrial Technology Research Institute, Hsinchu, Taiwan, R.O. China

Abstract—The effects of indium impurity on the etched morphology of high purity aluminium foils for electrolytic capacitor usage were investigated. The indium impurity was present either in as-received aluminium foils or deposited purposely on the foil surface through immersion-reduction reaction. The rolling line effect can be improved through introducing deposited indium on foil surfaces by immersion of the foil into $In(NO_3)_3$ solution prior to DC-etching. Under a high immersion temperature and more concentrated $In(NO_3)_3$ condition, surface etching competes with tunnel etching, and the foil thickness clearly decreases. Under low temperature and dilute $In(NO_3)_3$ condition, surface etching is inhibited and tunnel etching prevails. The different DC-etching behaviour under the two In-deposition conditions is explained through the energy state difference between the two deposited-In and the activation energy difference between surface etching and tunnel etching. The modification of etchability by indium on aluminium surface is stronger than that of lead. This facilitates employing lower temperature and dilute $In(NO_3)_3$ condition in the immersion-reduction process to optimize the etchability. © 1997 Elsevier Science Ltd

Keywords: A. aluminium, B. SEM, B. SIMS, C. pitting corrosion.

INTRODUCTION

The capacitance of electrolytic capacitors depends theoretically on the effective surface area of aluminium foil (electrode), the thickness of aluminium oxide film and the dielectric constant of the film. It is well known that an electrochemical etching process is an effective technique for increasing the surface area of aluminium electrode. For the capacitor size minimization and high voltage applications, vertical tunnel-type etching, rather than surface etching is demanded.

There are many factors which influence tunnel etching. The property of raw foils is one of the important factors. The well discussed properties of raw foil that influence the electrochemical etching process are grain size,[1] cubicity[2–4] and impurities or pre-existing flaws of the foil.[5–10] In general the grain size of aluminium foils for high voltage applications is relatively large, *ca.* 50 ~ 200 μm. A high cubic texture fraction (cubicity) is necessary for tunnel type etching because it has been shown that tunnels are formed preferentially along $<100>$ directions in hydrochloric acid.

The effect of impurity elements in aluminium foil, such as Fe, Cu, Si, Mg, Zn, etc. on tunnel etching has, also been well discussed. Arai[11] indicated that impurity elements, such as B and Bi in aluminium foil at the ppm level would prompt surface etching, i.e. inhibit tunnel formation, and result in decreased capacitance consequently.

Manuscript received 24 July 1996; in amended form 31 October 1996.

Much research[12,13] has indicated that the distribution of surface impurities could be even more important than impurity content. Some earlier work[14] focused on introducing trace elements, such as Fe and Cu, to increase initial etching sites and to enhance etchability (tunnel forming ability). The problem with introducing these elements is that the leakage current of their oxide film may increase significantly.

In the study on the etching of commercialized high purity aluminium foils for electrolytic capacitors, the origins of raw foils were found to influence the etching behaviour tremendously.[15] Under the same etching conditions, some foils produce uniformly distributed vertical tunnels while others undergo surface attack along rolling lines. In a previous report,[16] lead impurity on the aluminium foil surface was shown to exert significant influence on etching behaviour; the rolling line effect could be improved and etchability can also be increased through introducing deposited lead on to the foils. Recently, indium[17] was added to aluminium foil to improve the distribution of etching sites, but details were not revealed. Indium is very similar to lead in the chemical properties. Comparisons of this aspect between them were surveyed as follows:

Lead is in group IVA, and indium in group IIIA of the periodic table. Both lead and aluminium have a fcc structure, while that of indium is tetragonal. The atomic sizes of Pb ($r = 1.75$ Å) and In(1.66 Å) are relatively close, in comparison with the large difference between them and aluminium ($r = 1.43$ Å). Similar status occurs in the EMF values of the three elements (Pb: -0.13 V, In: -0.34 V, Al: -1.66 V). The overvoltage of hydrogen evolution on both lead and indium are relatively high[18]. Furthermore, the electronegativity values of indium and lead[19] (In:1.7, Pb:1.8) are almost the same. This is because both indium ($[Kr]4d^{10}5s^25p^1$) and lead ($[Xe]4f^{14}5d^{10}6s^26p^2$) have the d-orbital shield effect. According to Allred's report,[20,21] indium and lead have close ionization potentials (the three sequential ionization energies of indium are 5.79, 18.79, 27.90 eV, and those of lead are 7.41, 15.03, 32.00 eV). It can be found that the sum of the three ionization energies of indium (52.480 eV) and that of lead (54.445 eV) are very close. It implies that the immersion reduction of indium on aluminium ($In_{sol}^{3+} \rightarrow In_{Al}$) is very similar to that of lead on aluminium (Pb_{sol}^{2+} or $Pb_{sol}^{4+} \rightarrow Pb_{Al}$). The reason for considering the sum of the three ionization energies is because a certain portion of the lead cation is present as a divalency (Pb^{2+}) and the other portion is present as a tetravalency (Pb^{4+}) due to the lower promotion energy for $6s^26p^2 \rightarrow 6s^16p^3$ electron rearrangement, the mean valency of lead cation thus is three. The indium cation is present predominantly as a trivalency ($[Kr]4d^{10}5s^25p^1$).

In the previous report,[16] lead impurity has a significant effect on the etching behaviour of aluminium foils. The rolling line effect could be improved through introducing deposited lead on foil surface by immersion of the foil into $Pb(NO_3)_2$ solution prior to DC-etching and the etchability can be increased. In view of the above similarities between Pb and In it is suggested reasonably that indium would have similar effect on etchability as lead. It is interesting to study in detail the effect of indium impurity on the etching behaviour of commercialized aluminium foils in the present work.

EXPERIMENTAL METHOD

Raw aluminium foils

The raw foils (Foil A and Foil B) used in this work were high purity (99.99%) commercialized aluminium foils from two suppliers for high voltage application. The chemical compositions of the foils were determined by ICP-AES analysis and are shown in

Table 1. Chemical composition of the sample (wt ppm)

Element	Fe	Si	Cu	Mg	Zn	Mn	Cr	Ni	Ti	Pb	In
A	10.3	8.9	32.9	0.97	0.97	1.8	<1	<2	<1	<2	<30
B	8.9	8.5	27.5	1.20	5.0	1.9	<1	<2	<1	<2	<30

Table 1. The cubic texture fraction (cubicity) was determined with an X-ray diffractometer (Siemens-D5000) and the grain size of the foils was determined using image analyzer (Quantimet 520, Cambridge) after electro-polishing the foils. The experiment flowchart is shown in Fig. 1.

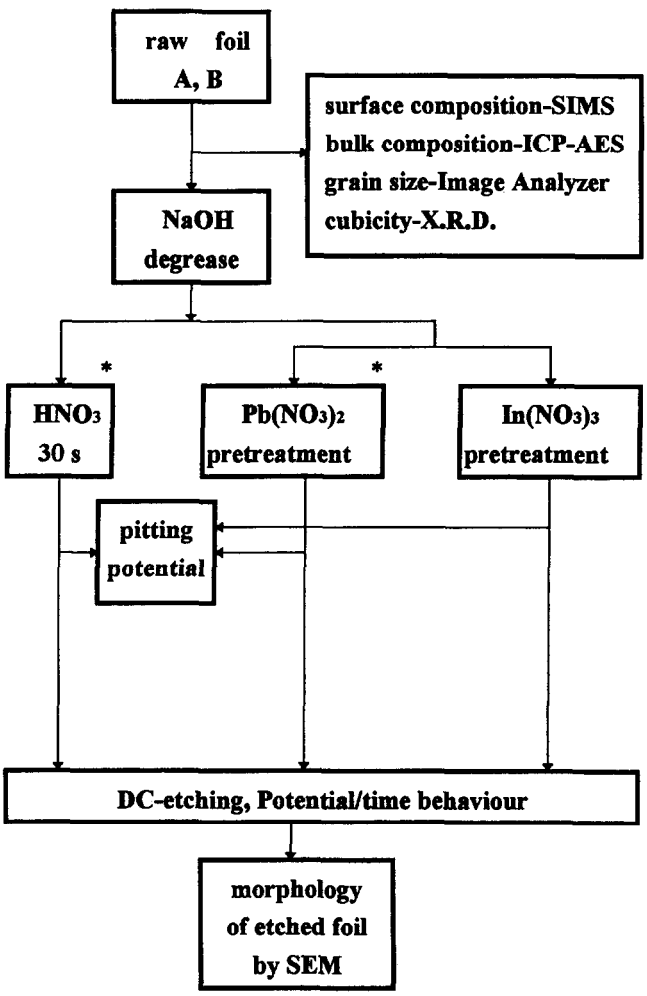

* previous report [16]

Fig. 1. Flowchart of the experimental procedure.

The depth profile of indium

Secondary ion mass spectrometry (SIMS, CMECA-IMS4F) was used to obtain the depth profiles of indium in the foils. The ion source is O^{2+} and the working current is 400 nA. The spot size is about 5 μm such that indium content in the rolling line can be characterized. The beam locations on the foils examined were rolling line areas and areas between rolling lines.

Pretreatment and DC-etching

Samples of dimension of 2 cm × 7 cm were degreased in 1N NaOH at 60°C for 60 s. After rinsing thoroughly with de-ionized water, the samples were immersed in 50% HNO_3 at 90°C for 30 s. Then the samples were rinsed with de-ionized water before being transferred to etching cell. For some experiments 0.1 N $In(NO_3)_3$ and 0.05 N $In(NO_3)_3$ instead of 50% HNO_3, at various temperatures were used to introduce indium on to the foil surface intentionally.

After pretreatments, samples were mounted on a sample holder with an area of 3 cm^2 exposed to the etching solution. The electrolyte used was 1 N HCl. All solutions used in this work were prepared from reagent grade chemicals and deionized water. A high purity (99.95%), high density graphite was used as a counter electrode. A reference electrode (Ag/AgCl/3 M KCl) was placed at fixed position behind the sample holder. All potentials reported in this work are referred to this reference electrode.

Direct current (DC) etching was carried out immediately after placing the sample holder into the electrolyte. The current density was 200 mA/cm^2 and applied typically for 1 s and 20 s at 70°C. A potentiostat/galvanostat (Princeton Applied Research, PAR273), interfaced to a personal computer, was used to supply constant current as well as to measure pitting potential. Pitting potentials of specimens after different pretreatments were measured, in 1 N HCl at 70°C, through cyclic voltammetry technique with a scan rate of 20 mV/min.

Etched morphology observation

After electrochemical etching, the samples were rinsed with de-ionized water, dried in ambient conditions. For surface morphology studies, the samples were sputter-coated with gold before examining in a scanning electron microscope (SEM, Hitachi-2500). For sectional observation, which would shed lights on tunnel development, the etched samples were anodized, mounted vertically in epoxy resin, mechanically polished, chemically dissolved, sputter-coated with gold and examined under SEM. Details of the above procedure are given elsewhere.[22]

Foil thickness measurement

The thickness of pretreated and/or DC-etched foils were measured using electronic micrometer, with precision to ±0.5 μm, as well as measured from the SEM cross-section views of foils.

EXPERIMENTAL RESULTS

Surface composition analysis

Secondary ion mass spectrometer (SIMS) was used to characterize the surface composition and depth profiles of elements in as-received aluminium foils.

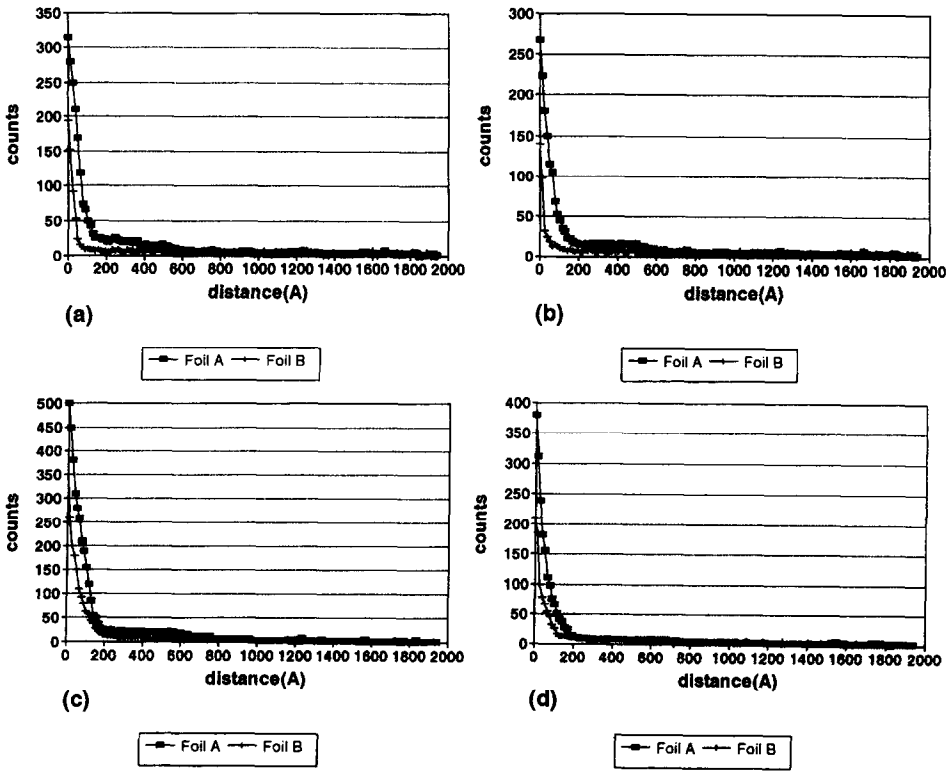

Fig. 2. The depth profiles of indium of two foils: (a) as-received, on the rolling line; (b) as-received, between the rolling line; (c) after $NaOH/HNO_3$ treatment, on the rolling line; (d) after $NaOH/HNO_3$ treatment, between the rolling line.

Figures 2(a) and 2(b) are the depth profiles of indium located on rolling lines and between rolling lines, respectively. Figure 2 shows clearly that for all locations, the concentration of indium in Foil A is greater than that in Foil B. Figure 2 also shows that indium is enriched in the surface layer (to *ca.* 300-500 Å in depth) and approached null beneath the enriched layer. There is no difference in indium concentration for the two foils in the inner section.

Figures 2(c) and 2(d) are the depth profiles of indium located on rolling lines and between rolling lines, respectively, after a $NaOH/HNO_3$ pretreatment. The surface and in depth distributions of indium in both regions are very similar to those of as-received foil.

Etched morphologies with HNO_3 pretreatment

To study further differences of Foil A and Foil B, the two foils were degreased with 1N NaOH, pretreated with 50% HNO_3 and then etched with direct current at 200 mA/cm^2 for different times. This results were reported in the previous study[16] which shows that rolling line effect, i.e. the effect which results in concentrated etching pits along rolling lines leaving vast areas in between unattacked, are observed for both foils after short time etching (1 s). The rolling line effect is more serious in Foil A than that in Foil B. The surface etching, instead of tunnel etching, prevail on both foils even after etching for 20 s.

In the literature, the effects of impurities in aluminium foil on electrochemical etching process have been reported. It was found that the kind of impurities as well as their distributions have great influence on the etching behaviour. Other properties of the raw foil, such as grain size and cubicity, have also been mentioned. In the present work, the cubicity and grain size of the two foils were measured. The differences in grain size (180 μm for Foil A, 200 μm for Foil B) and cubicity (90.5% for A, 89.0% for B) are relatively small between the two foils, implying that they are not the major factors responsible for the surface morphology difference between the two etched foils. It is suggested that the difference of rolling line effect in the two foils results from the amount and kinds of segregation impurity such as lead and indium on rolling line.

Etched surface morphologies with $In(NO_3)_3$ pretreatment

To understand further the effect of indium on the electrochemical etching behavior, indium was introduced intentionally on to the foil. The two foils were degreased with NaOH, pretreated with 0.1 N $In(NO_3)_3$ at 90°C for 30 s and then DC-etched typically for 1 s and 20 s. Apparent gas bubbles evolved on the foil surface before the passage of etching current. These bubbles quite possibly arose from the chemical etching reaction when the foils were dipped in etching solution. The etched surface morphologies for both Foil A and Foil B are shown in Figs 3 and 4, and the corresponding cross-section views are shown in Figs 5 and 6, respectively. It is clear from Figs 3 and 4 that $In(NO_3)_3$ pretreatment changes tremendously the etching behavior of both Foil A and Foil B. The rolling line effect disappeared clearly and pits were distributed uniformly over the two foil surfaces even after etching for 1 s. A cross-section micrograph (Figs 5 and 6) shows that most of the etching pits, or tunnels, grew perpendicular to the foil surface, and increased in length with etching time. The measured thickness of foils decreases clearly (Fig. 5: 106 μm–93 μm for Foil A,

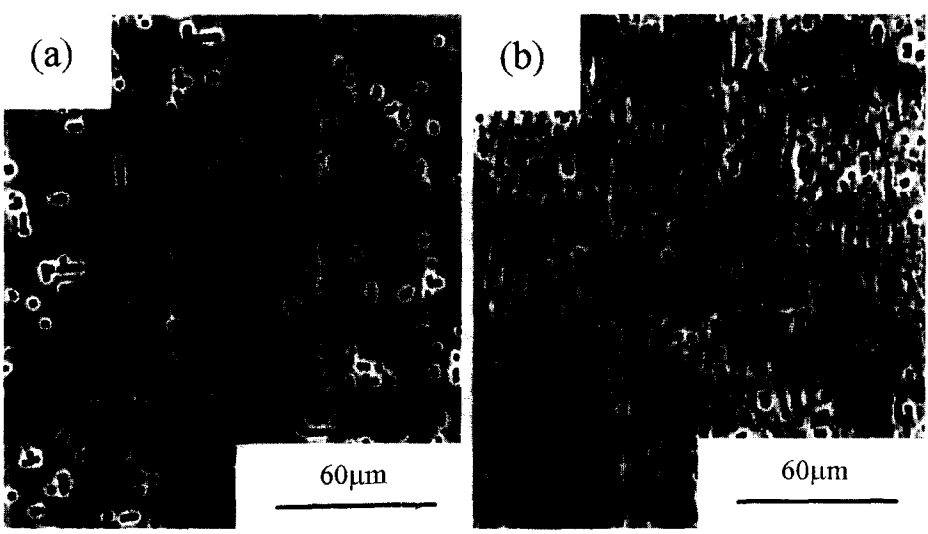

Fig. 3. Surface morphologies of Foil A, pretreated in 0.1 N $In(NO_3)_3$ for 30 s, DC-etched for (a) 1 s, (b) 20 s.

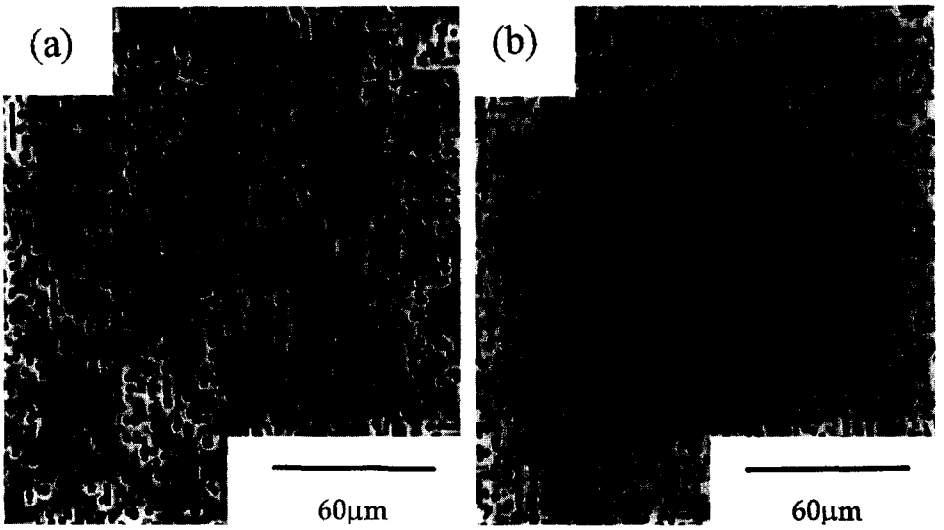

Fig. 4. Surface morphologies of Foil B, pretreated in 0.1 N $In(NO_3)_3$ for 30 s, DC-etched for (a) 1 s, (b) 20 s.

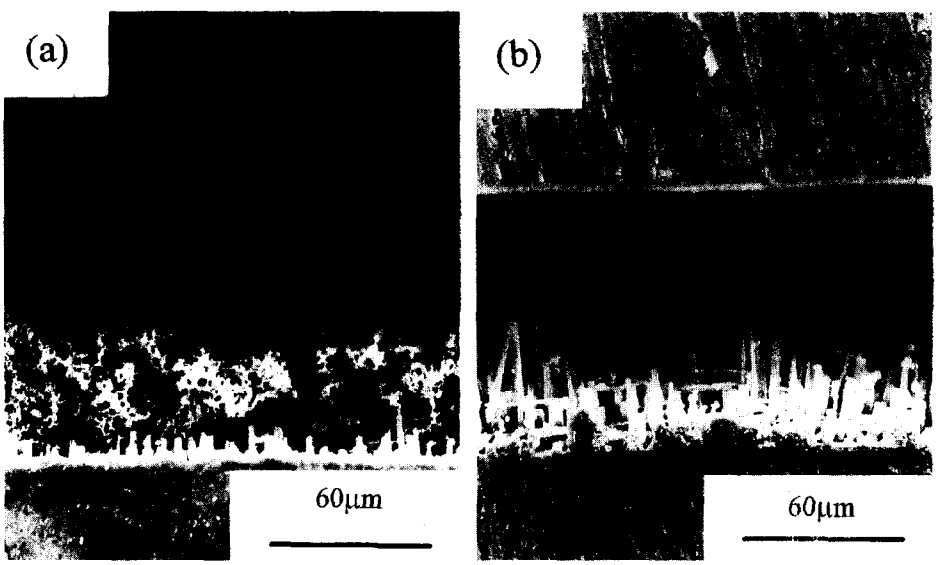

Fig. 5. Cross-section view of Foil A, pretreated in 0.1 N $In(NO_3)_3$ for 30 s, DC-etched for (a) 1 s, (b) 20 s.

Fig. 6: 103 μm–90 μm for Foil B), implying that surface etching also happened during DC-etching.

An experiment which shows chemical etching is not so obvious prior to DC-etching was performed on Foil B. In the experiment, the concentration of $In(NO_3)_3$ was diluted to 0.05 N, the immersion temperature was lowered to 40°C; Foil B was then immersed in the etching solution for 30 s prior to DC-etching. The rolling line effect can be improved to increase tunnel forming ability with 0.05 N $In(NO_3)_3$ pretreatment. As shown in Fig. 7, the

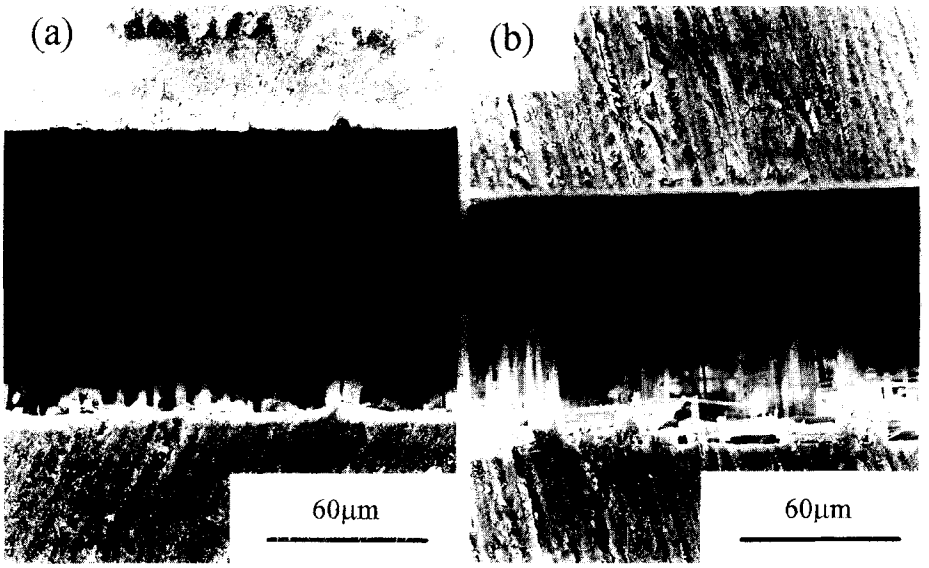

Fig. 6. Cross-section view of Foil B, pretreated in 0.1 N $In(NO_3)_3$ for 30 s, DC-etched for (a) 1 s, (b) 20 s.

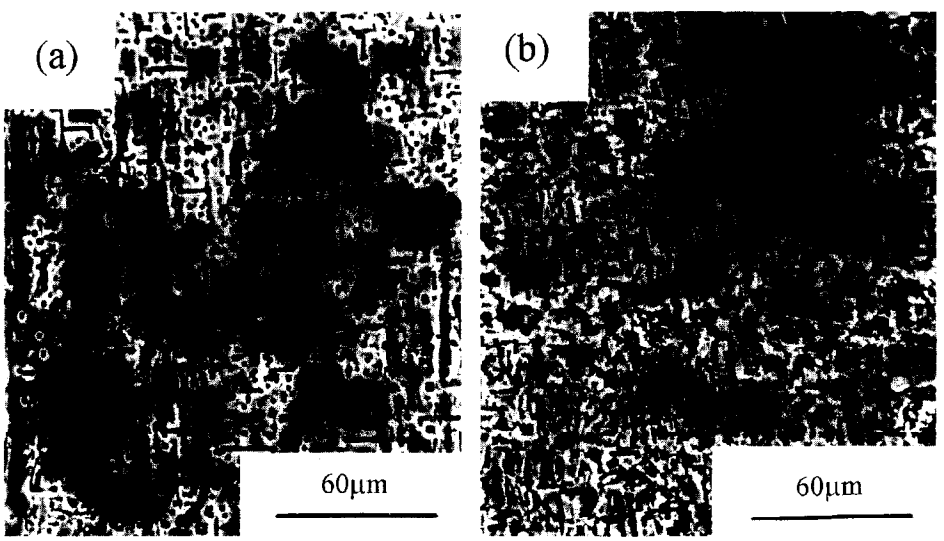

Fig. 7. Surface morphologies of Foil B, pretreated in 0.05 N $In(NO_3)_3$ for 30 s, DC-etched for (a) 1 s, (b) 20 s.

etching pits on Foil B are distributed uniformly over the entire surface for etching times as short as 1 s. The corresponding cross-section view in Fig. 8 shows clearly that most of the etchings were tunnel type. The tunnel density seems higher than that pretreated with 0.1 N $In(NO_3)_3$ (comparing Fig. 6 with Fig. 8). The thickness of foils does not decrease obviously. It implies that surface etching was inhibited and tunnel etching prevailed.

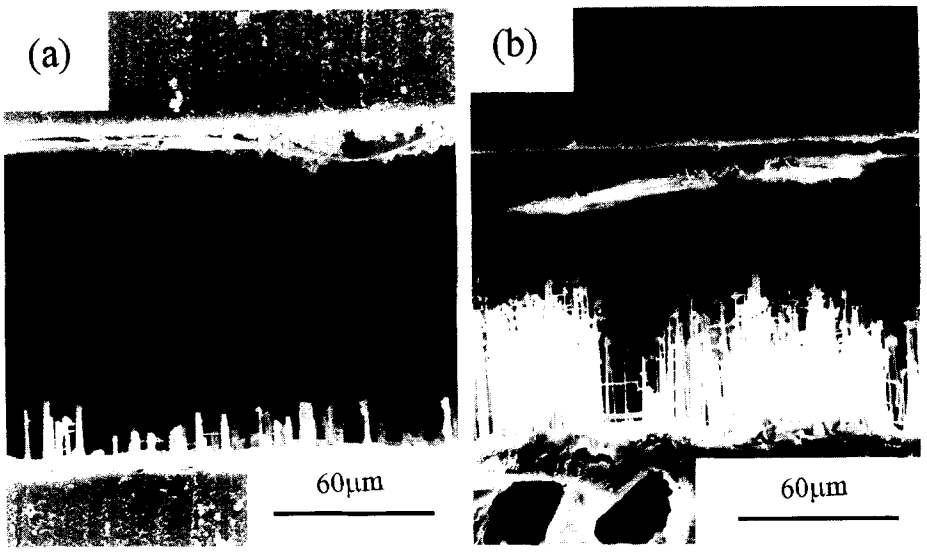

Fig. 8. Cross-section view of Foil B, pretreated in 0.05 N $In(NO_3)_3$ for 30 s, DC-etched for (a) 1 s, (b) 20 s.

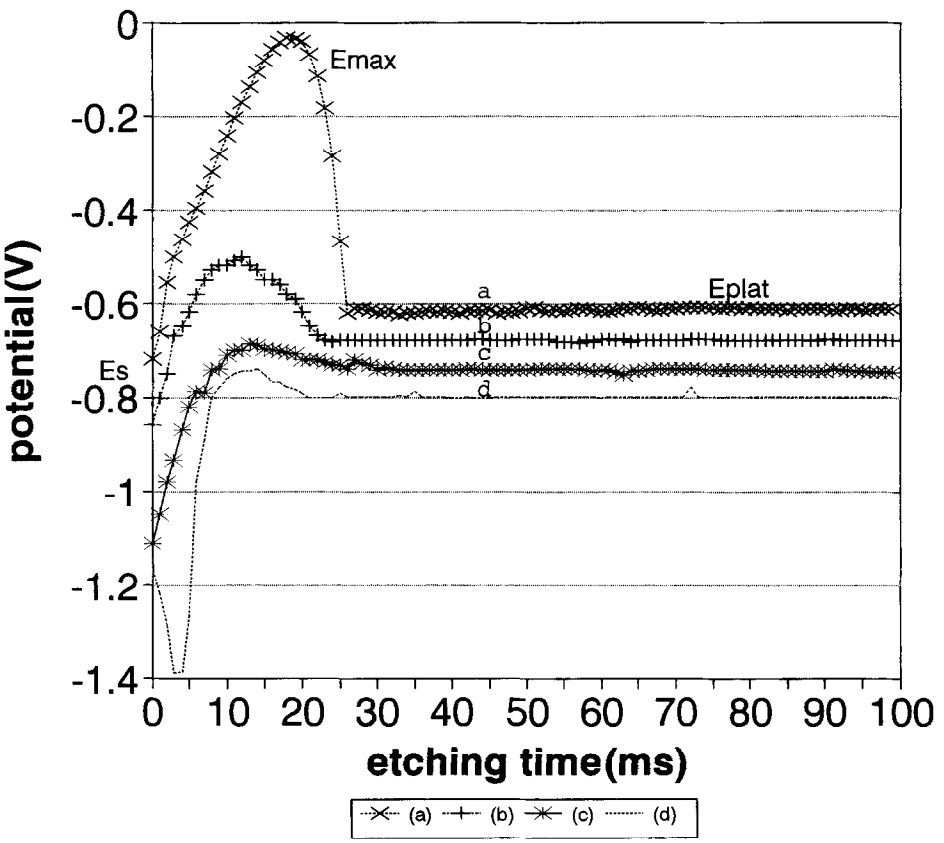

Fig. 9. The potential-time behaviour during DC-etching of Foil B with (a) $NaOH/HNO_3$, (b) $NaOH/Pb(NO_3)_2$, (c) $NaOH/0.05$ N $In(NO_3)_3$, (d) $NaOH/0.1$ N $In(NO_3)_3$ pretreatments.

Pitting potential

The pitting potential for Foil A and Foil B with HNO_3 pretreatment are found to be -0.98 V and -1.00 V (Ag/AgCl), respectively. The effect of $In(NO_3)_3$ treatment on pitting potentials of the two foils was also studied. For Foil A, which has higher as-received indium content, the indium introducing pretreatment resulted in a shift of pitting potential from -0.98 V to -1.15 V. The pitting potential for Foil B, with lower as-received indium content, shifts from -1.00 V to 1.17 V.

Potential-time behaviour

The recorded potential-time behaviour during DC-etching of variously pretreated Foil B are shown in Fig. 9. The characteristic features of each curve are: (a) there is a starting surging potential (E_s), and (b) the potential continues to increase from E_s to a maximum value (E_{max}), and then decreases gradually to a plateau value (E_{plat}).

One exception exists in curve d, which shows a downward potential inversion peak in the E_s-E_{max} stage.

DISCUSSION

Rolling line effect in HNO_3-pretreated foil

The previous report[16] shows that for both types of foils with HNO_3 pretreatment, most of the etching pits are created along rolling lines. Rolling lines are high strain area. Much research has indicated that there are high concentrations of impurities, such as lead and indium, and dislocations distributed along rolling lines. It is believed that these highly concentrated defects in rolling lines would serve as the major sites for pit initiation. The impurity segregation on rolling lines may have been resulted from stress-driven solid state diffusion during rolling. In a previous study of lead impurity, it is concluded that the rolling line effect was related partly to the content of lead in foils. In addition to lead, indium may also be one of sources which would result in rolling line effect. In the present work, SIMS measurements show that the indium impurity also being concentrated in rolling line, and the indium peak of Foil A is higher than that of Foil B (Fig. 2).

The rolling line effect is related partly to the content of impurity such as indium and lead in foils. For example, Foil A, which has higher indium and lead content, has stronger rolling line effect than Foil B. For HNO_3 pretreated foils, it is observed that the rolling line effect still occurs on Foil A after etching for 20 s, whereas the rolling line effect does not occur so apparently for Foil B.[16] This is because the emf value of indium is much higher than that of aluminium; during the electrochemical etching process, indium plays as a cathode and aluminium as an anode. Indium and aluminium form a local cell. The etchings initiate at the sites where the larger local cells exist, i.e. along the rolling line, which provide larger driving force. For the foil with lower indium content, etchings start along rolling lines and then spread over in between rolling lines as etching time increases. On the other hand, the foil with the higher indium content would possibly produce more local cells along rolling lines. Consequently, etchings are mainly located along rolling lines. Concerning the above reasoning, one may argue that indium contained in the bulk metal could be once dissolved and then redeposited, thus the surface and in depth distributions of indium could be varied after $NaOH/HNO_3$ treatment. The argument is clarified in Fig. 2c and 2d, which shows the surface and in depth distributions along and in between rolling lines are very similar to those of as-received foil (Fig. 2a and 2b). The same behaviour occurs with lead impurity as

reported in the previous study.[16] This concludes that the concentrations of indium and lead in Foil A, both surface and in depth and both along and in between rolling lines, may be dominantly responsible for the more serious rolling line effect appeared in DC-etched Foil A after $NaOH/HNO_3$ treatment. However, it is difficult to identify which is more effective on the rolling line effect between lead and indium due to the lack of ppm grade impurity standards. The answer to this question seems can only be deduced implicitly from the behaviour of deposited indium through $In(NO_3)_3$ pretreatment.

Improved etchability by $In(NO_3)_3$ than $Pb(NO_3)_2$ pretreatments

In the study of lead impurity effect, for foils with a higher concentration of lead, there are more lattice strain sites both in rolling line and in between rolling lines. In the present work, the modification of etchability by indium on aluminium surface seems stronger than that of lead under the same immersion reduction condition. The rolling line effect disappears on both types of foils by introducing indium on aluminium surface.

For both type foils, the rolling line effect can be improved to increase tunnel forming ability with introducing of 0.1 N $In(NO_3)_3$ pretreatment. As shown in Figs 3 and 4, the etching pits are distributed uniformly over entire surface for etching time as short as 1 s. The corresponding cross-section views in Figs 5 and 6 show that a little more tunnel type etching pits form with an obvious decrease in foil thickness (*ca.* 106 μm–93 μm for Foil A and 103 μm–90 μm for Foil B); the latter effect hampers the improved etchability.

It was found that chemical etching occurred on the aluminium surface with 0.1 N $In(NO_3)_3$ pretreatment before passing current since gas bubbles were observed. This may be caused by the stronger In//Al local cells and chemical etching occurs in HCl solution. It is reckoned that since indium belongs to IIIA group, the chemical properties of indium are largely determined by the behaviour of the incomplete outer electronic shell, which consists of two 5s and one 5p electrons ($5s^2 5p^1$). That is to say indium has affinity to Cl^- due to the empty orbital (i.e. empty p-orbital) which would facilitate adsorption of Cl^- on aluminium/indium interface and aluminium surface. The Cl^- adsorption would accelerate dissolution of aluminium and/or hydration of Al^{+++} into bulk solution and result in a decreased pitting potential (chemi-sorbed theory),[23,24] i.e. toward more active direction. The pitting potentials shift toward more active direction as a consequence of indium reduction after immersing in $In(NO_3)_3$ than those in $Pb(NO_3)_2$.[16]

The reaction of deposited indium with hydrochloric acid is favored by the complexing reaction: Al/In (volume enclosed deposited indium are active sites)$\rightarrow Al^{+++}$ and In^{+++}

$$In^{+++} + Cl^- \rightarrow \text{indium chloride complex}^{25}$$

The soluble indium chloride complexes would further result in serious surface corrosion due to the decrease of activation polarization energy of aluminium surface by adsorption of indium chloride complexes during DC-etching. This effect is similar to that effect of Cl^- on the aluminium surface and the indium complexes would exert a larger effect than Cl^- due to its larger size.[26] This makes a reduced selectivity on the reaction sites, and would increase surface etching (i.e. a decrease the foil thickness).

Concerning the above reasoning, one may question the role, cathodic or anodic, played by indium. Deposited indium is a second phase inherent as-received indium in raw foils, is in solid solution in high purity (99.99%) aluminium. The H^+ reduction is favorable on the solid solution state indium since in this case the overall reduction surface energy and lattice is close to those of pure aluminium, thus the activation energy of H^+ reduction is low.

Indium therefore acts as a cathode relative to aluminium matrix in the etching process. Deposited indium tends to act as an anode due to (1) the high hydrogen reduction overvoltage on exposed second phase indium and (2) the easy complexing of chloride with indium.

The recorded potential-time behaviour during DC-etching of Foil B is shown in Fig. 9. Figure 9a–d are the potential-time plots with $NaOH/HNO_3$, $NaOH/Pb(NO_3)_2$, $NaOH/0.05\ N\ In(NO_3)_3$, $NaOH/0.1\ N\ In(NO_3)_3$ pretreatments, respectively. As shown in Fig. 9a–c three stages can be found on each curve:(1) E_s-E_{max} stage, (2) E_{max}-E_{plat} stage, and (3) E_{plat} stage. Among the curves, the one with $NaOH/HNO_3$ pretreatment is most noble, that with $NaOH/0.1\ N\ In(NO_3)_3$ pretreatment is most active, leaving that with $NaOH/Pb(NO_3)_2$ and $NaOH/0.05\ N\ In(NO_3)_3$ pretreatments in between. This may be due to different surface modification status caused by various pretreatments. The effect of indium on aluminium foil is stronger than that by other pretreatments and the In//Al local cells drive the potential in the active direction. As Fig. 9d shown, there is a peculiar downward potential inversion peak in the E_s-E_{max} stage. It is suggested that the stronger In//Al local cells are responsible to the inversion peak.

Further illustration of the In-deposition effect

Figure 10 is a schematic energy state diagram of the etching to explain the above observation. As shown in the diagram, proper amounts of dispersed deposited indium aid in tunnel etching due to a lower activation energy for tunnel etching ($\Delta G^*_{f\to b}$)., i.e. path b is more likely than path a for low temperature and dilute $In(NO_3)_3$ pretreatment. For high temperature and concentrated $In(NO_3)_3$ pretreatment, greater amounts of indium is reduced on to aluminium would decrease in thickness of the foil obviously since surface etching is in competition with tunnel etching as seen in Fig. 10, i.e. $\Delta G^*_{g\to a}$ and $\Delta G^*_{g\to b}$ are more comparable, than $\Delta G^*_{f\to a}$ and $\Delta G^*_{f\to b}$, to overcome.

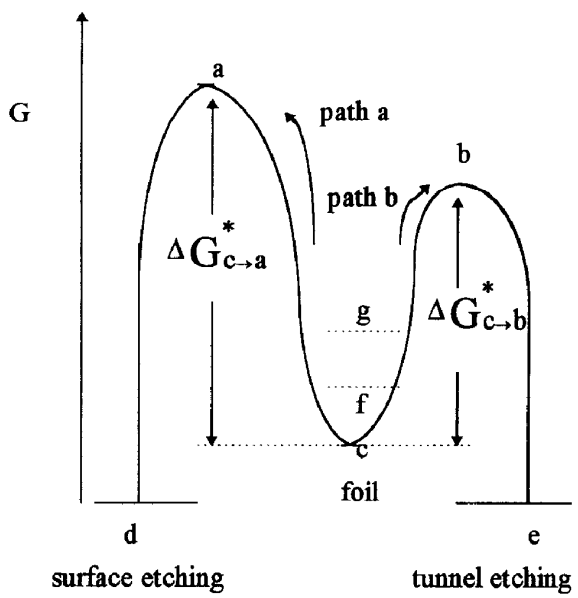

Fig. 10. The schematic energy state diagram of the etchings.

It should be noted that Fig. 10 is invalid under the situation that foil thinning is caused by the merging or connecting of a number of small tunnel pits all over the surface due to very high population density of pits induced by very high amount deposited indium on aluminium. In this case, it is difficult to distinguish between tunnel etching and surface etching since tunnel etching also plays a role to decrease the foil thickness.

CONCLUSIONS

(1) The rolling line effect can be improved through introducing deposited indium on foil surface by immersion of the foil into $In(NO_3)_3$ solution prior to DC-etching. Under high immersion temperature and more concentrated $In(NO_3)_3$ condition, surface etching competes with tunnel etching, and the foil thickness decreases obviously due to more indium deposition and the as-formed strong and adjacent In//Al local cells. Under low temperature and dilute $In(NO_3)_3$ condition, surface etching is inhibited and tunnel etching prevails. The different DC-etching behaviours under the two In-deposition conditions are explained through the energy state differences between the two deposited-In and activation energy difference between surface etching and tunnel etching.

(2) The modification of etchability by indium on aluminium surface is stronger than that of lead. This facilitates employing lower temperature and dilute $In(NO_3)_3$ condition in the immersion-reduction process to optimize the etchability.

REFERENCES

1. K. Arai and T. Suzuki, *Light Metal* **31**, 675 (1981).
2. R. Bakish, E.Z. Border and R.J. Kornhass, *J. Electrochem. Soc.* **109**, 791 (1962).
3. R. Bakish, *Electrochem. Technol.* **6**, 192 (1968).
4. Z.Q. Zheng and W.B. Zhang, *J. China Inst. South Inst. Mining Central Metal* **1**, 111 (1983).
5. R. Bakish, R.J. Kornhass and E.Z. Border, *J. Electrochem. Soc.* **1**, 358 (1963).
6. O. Scri, *Surface Tech.* **44**, 23 (1993).
7. R.B. Diegle, *J. Electrochem. Soc.* **121**, 583 (1974).
8. G. Muriset, *ibid.* 1952, **99**, 285.
9. L.V. Alphen, P. Nauwen and L. Slakhorst, *Z. Metallkd.* **70**, 158 (1979).
10. G.E. Thompson and G.C. Wood, *Corros. Sci.* **8**, 721 (1978).
11. K. Araii, T. Suzaki and T. Atsumi, *J. Electrochem. Soc.* **132**, 1667 (1985).
12. H. Biloni, M.F. Bolling and H.A. Domain, *TMS-AIME* **233**, 1926 (1965).
13. A.P. Bond, M.F. Bolling and H.A. Domain, Tech. Rep. No. SL-65-50, Ford Motor Company Science Laboratory, 1965.
14. I. Nagata, *Aluminium Electrolytic Capacitor*. Japan Chemical Condensor Corp. 1983, p. 186.
15. W. Lin, G.C. Tu, C.F. Lin and Y.M. Peng, unpublished work.
16. W. Lin, G.C. Tu, C.F. Lin and Y.M. Peng, *Corros. Sci.* **38**, 889 (1996).
17. K. Fukuoka and M. Kurahashi, *The Electrochemical Society of Japan Conf*, Fukwoka, 1993.
18. Data from B.E. Conway, *Electrochemical Data*. Elsevier, New York, 1952.
19. W.D. Callister, *Materials Science and Engineering*, 2nd edn. Wiley, New York, 1991, p. 16.
20. R.S. Drago, *J. Phys. Chem.* **62**, 153 (1958).
21. A.L. Allred and E.G. Rochow, *J. Inorg. Nucl. Chem.* **5**, 264 (1958).
22. C.G. Dunn, R.B. Bolon, A.S. Alwan and A.W. Stirling, *J. Electrochem. Soc.* **118**, 381 (1971).
23. T.P. Hoar and W.R. Jocob, *Nature* **216**, 1299 (1967).
24. H.H. Uhilig and H. Böhni, *J. Electrochem. Soc.* **116**, 906 (1969).
25. T. Spiro, *Inorg. Chem.* **4**, 1290 (1965).
26. J. Bockris and A.K.N. Reddy, *Modern Electrochemistry*. Plenum, New York, 1977, pp. 742–745.